Sensors and Actuators B 147 (2010) 475–480

Contents lists available at ScienceDirect

Sensors and Actuators B: Chemical

journal homepage: www.elsevier.com/locate/snb

# Cancer marker detection in human serum with a point-of-care low-cost system

Pasquale Grosso [a], Sandro Carrara [b,*], Claudio Stagni [a], Luca Benini [a]

[a] D.E.I.S. Department, Bologna University, Italy
[b] EPFL - Swiss Federal Institute of Technology Lausanne, Switzerland

ARTICLE INFO

*Article history:*
Received 11 November 2009
Received in revised form 1 April 2010
Accepted 2 April 2010
Available online 18 April 2010

*Keywords:*
Low-cost photodiodes
Chemiluminescence
ELISA assay
Immunoassay
Point-of-care

ABSTRACT

Chemiluminescence, i.e. the emission of light from a chemical reaction, offers interesting opportunities for developing point-of-care biosensors. However, commercially available systems are expensive, bulky, and primarily addressed to laboratory usage. The goal of this paper is to present a novel work related to the design and experimental validation of a point-of-care device for cancer marker detection in human serum. The new system has been especially developed for cost-sensitive applications using only low-cost off-the-shelf components. The system was tested with blood serum. The output signal from spots with specific proteins uptake was two orders of magnitude higher than that from control spots: it was $14 \pm 3$ mV/s from the detection spots, while it was only 260 μV/s and 242 μV/s from the control spots.


## 1. Introduction

The interest in chemiluminescence assays increased very rapidly in the last decades. This detection technique enables chemical and biochemical tests. It is very flexible, and it achieves a sensitivity of few pMol [1]. Hence, it has been used for detection of explosives [2], environmental control of soil and dusts [3], screening in food [4], bacteria identification [5], biohazard applications [6], and for medical diagnostics [7,8]. The new frontier in diagnosis is point-of-care testing. It is defined as a testing at or near the site of patient care [9]. In this context, a distinctive advantage of chemiluminescence with respect to fluorescence and other optical techniques is the absence of external light sources, which significantly simplifies the implementation of detection systems [10]. However, the available chemiluminescence detectors used in laboratory practice are still expensive and bulky. Therefore, they are not suitable for hand-held point-of-care usage. A point-of-care usage requires small and low-cost detectors. Size reduction is not a big issue, since single-chip approaches were already proposed in 1997 [11]. Recently, an applications-specific integrated circuit (ASIC) was developed with an array of 128 detectors [6]. However, such ASIC still have very significant costs in terms of non-recurrent engineering and production. Further cost reduction might come from amorphous silicon [12], but design-related costs will remain high due to a not so large and the extremely high level of parallelism in the essay. On the other hand, Xin et al. reported quantitative determinations of molecules by chemiluminescence directly in human serum [13]. In particular, the aim was the detection of cancer markers. Despite aggressive treatments, it was demonstrated that cancer patients have less than 5-year survival time if diagnosis is made at an advanced stage. On the contrary, patients have higher chances if cancer is diagnosed in an earlier stage [14]. However, the current methods to detect cancer markers using chemiluminescence are based on lab scanners, which are cumbersome, slow, and highly expensive. These limitations affect the early detection of cancer formation. Therefore, the development of low-cost devices is still required to improve cancer diagnosis. Label-free techniques were proposed as alternative to chemiluminescence, but they are still under development and their sensitivity is still too low to efficiently detect cancer markers in patient's samples [15]. On the other hand, the ELISA test based on chemiluminescence remains the best technique for early cancer detection. Therefore, optical point-of-care devices are urgently required to replace ELISA test, more expensive and complex, in order to perform diagnosis directly to the hospital. Recently, Xu et al. [16] proposed a low-cost optical based on photomultipliers, but not suitable for point-of-care arrays. The aim of the present paper is to illustrate a novel and successful design for a point-of-care system, developed on board with low parallelism (i.e. 2–8 detectors), very low-cost and off-the-shelf components. The proposed solution is the best trade-off among low-volume, cost-sensitive markets and limited parallelism essay.

## 2. Materials and methods

The following section describes system architectures and related materials for test and validation of the developed device

* Corresponding author.
*E-mail address:* sandro.carrara@epfl.ch (S. Carrara).

0925-4005/$ – see front matter © 2010 Elsevier B.V. All rights reserved.
doi:10.1016/j.snb.2010.04.001

for chemiluminescent measurements. Two different solutions were tested for signal amplification and conditioning. A PC plug-in LabVIEW (National Instruments Inc., Austin, TX) Data Acquisition board was used to acquire signals and a simple LabVIEW program was developed to test the two different architectures.

### 2.1. Choice of the detector

Regarding the choice of the detector, the goal is to detect feeble light generated by a chemiluminescent reaction. Photoemission rate can be extremely low, down to $4 \times 10^5$ photons/cm$^2$ s ($1.65 \times 10^{-12}$ W/cm$^2$) at emission wavelength of 480 nm. Although the choice of an optical detector is often complex, some key factors should be considered: quantum efficiency (QE), sensitivity, active area, minimum acceptable signal-to-noise ratio (SNR) and cost. Quantum efficiency is really important, since it is the ratio between the number of electrons (or holes) generated as photocurrent and the number of the incident photons. However, more often the SNR is the most important feature used to choose the detector. In fact, the noise of the detector has some components proportional to the signal and others independent from the signal. The independent components consist of thermal noise (or Johnson noise) and dark current noise. The Johnson noise ($i_j$) is typical of solid-state detectors, like avalanche photodiodes (APDs) and photodiodes (PDs), and it can be described by

$$i_j = \left(\frac{4kTB}{R_{sh}}\right)^{1/2} \quad (1)$$

where $k$ is the Boltzman constant, $T$ is the absolute temperature, $B$ is the frequency bandwidth and $R_{sh}$ is the shunt resistance. The dark current noise, or dark current shot noise, ($i_{sd}$) is expressed as follows:

$$i_{sd} = (2qI_dB)^{1/2} \quad (2)$$

where $q$ is the electron charge and $I_d$ is the dark current. On the other hand, component depending on the signal is typically due to statistical fluctuations:

$$i_{SS} = (2qI_SB)^{1/2} \quad (3)$$

where $I_S$ is the photocurrent generated by the photoelectric effect. Then, all these components contribute to SNR as:

$$\mathrm{SNR} = \frac{I_S}{(i_j^2 + i_{SD}^2 + i_{SS}^2)^{1/2}} = \frac{I_S}{(4KBT/R_{sh} + 2qI_DB + 2qI_SB)^{1/2}} \quad (4)$$

Further noise source can come from non-specific molecular binding, like interfering molecules that adhere non-specifically to the sensing surface. This noise is not specifically related to the detection, or to photodetectors. Indeed, it is related to properties of the sensing, and, in particular, to its nano-scale features [17]. Improvements to avoid non-specific molecular binding are usually addressed by considering poly(ethylene glycol) (PEG), for coating clean ELISA glass slides [18]. About photodetector-related noise, a comparison was performed among different responses of commercially available systems, aiming to identify the key parameters of the detector in real systems. This comparison was done using a simple reaction of enhanced chemiluminescence (samples with 45 μL of luminol reagent, 45 μL of oxidizing reagent (HRP) and 10 μL of IGM–HRP conjugate). Three commonly-used systems were considered to check the performances of the photodetector. The first was a Luminoskan (ThermoFisher Scientific Inc., Waltham, MA) based on photo-multiplayer detectors. The second was a Kodak Image station 4000 R – Chemidoc (Carestream Health Inc., formerly Kodak Molecular Imaging Systems, Rochester, NY) based on a low noise type of cooled CCD with high level of sensitivity in a wavelength region of 400–550 nm. The third was a Scanner Storm 860

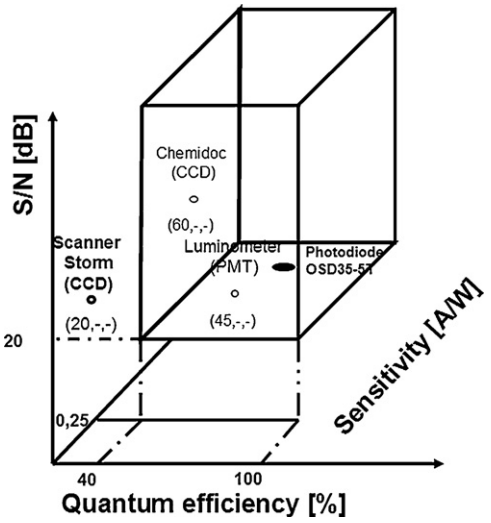


**Fig. 1.** Comparison of tested photo-detector characteristics and the limits box required to detect chemiluminescent signals.

Molecular Imager (Molecular Dynamics Inc., Sunnyvale, CA), which is a CCD system with low quantum efficiency (20%) at 480 nm. The chosen photodetector to test was the commercial photodiode OSD35-5T (OSI Optoelectronics, Hawthorne, CA), which presents high quantum efficiency (64%) and sensitivity (0.25 A/W) at a wavelength of 480 nm. Fig. 1 summarizes different photo-detection systems, showing that a quantum efficiency higher than 40% at 480 nm, a sensitivity higher than 0.25 A/W and a signal-to-noise ratio higher than 20 dB are required to detect a chemiluminescent emission. Therefore, the photodiode OSD35-5T was chosen for our application. It has a good signal-to-noise ratio, excellent quantum efficiency (60%) and a good sensitivity (0.25 A/W) at 480 nm. Moreover, photodiodes have also an excellent linearity of output current, as a function of the incident light. This kind of photodiodes do not require high voltages and they are suitable for dense arrays. Furthermore, they are cheaper compared with avalanche photodiodes and other high-sensitivity detectors.

### 2.2. Signal conditioning architectures

Two circuits were designed and compared. The first light detection circuit (Fig. 2) presents a high-speed current-to-voltage conversion operational amplifier. The incident photons onto the photodetector are converted into a photocurrent $i_{ph}$. An operational amplifier is required to develop the current-to-voltage converter in order to acquire weak signals. The output voltage $V_o$ is directly

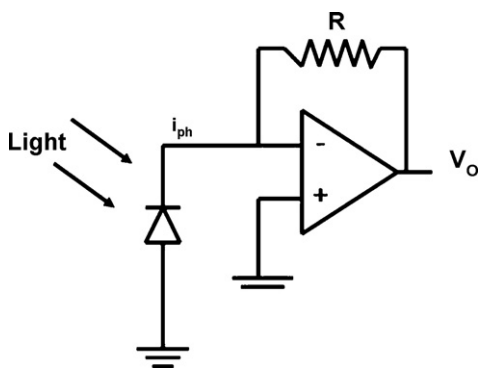


**Fig. 2.** Circuit architecture proposed with a photodiode and a trans-impedance amplifier.

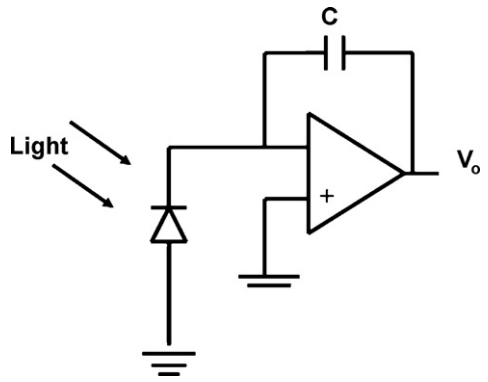


**Fig. 3.** Circuit architecture proposed with a photodiode and an operational amplifier integrator.

related to the generated current:

$$V_o = i_{ph}R \quad (5)$$

The second detection circuit presents an integrator circuit (Fig. 3). In this second architecture, the photocurrent generated by incident photons charges a capacitor. The amount of charge is limited by the diffusion well capacity. The average photocurrent is obtained from the integration of the output voltage $V_o$ across the capacitance $C$ over the time. A low dielectric absorption capacitor is used to suppress reset errors.

### 2.3. System on board

Two printed circuit boards (PCB) are designed and fabricated to implement the two aforementioned configurations. The boards present two levels of copper (top and bottom sides of the board). Components placement is chosen in order to minimize the occupied area and to support critical contacts. Fig. 4 shows the current-to-voltage conversion board and the related space available for housing a typical ELISA test glass slide. A DC voltage of 12 V is the input voltage. The operational amplifier OPA 111 works with dual supply power of ±5 V. Component TEN 1221 (Traco Power) is used to generate the three reference voltages of +5 V, −5 V and ground. Photodiodes are connected between the two inputs of the trans-impedance amplifiers. They are polarized with 0 V and, thus, they

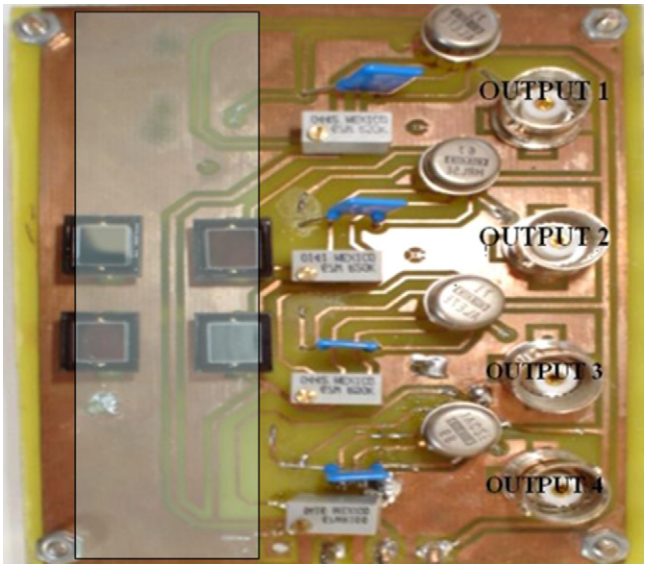


**Fig. 4.** Current-to-voltage conversion board. The image also schematically shows housing of typical glass slide used in ELISA tests.

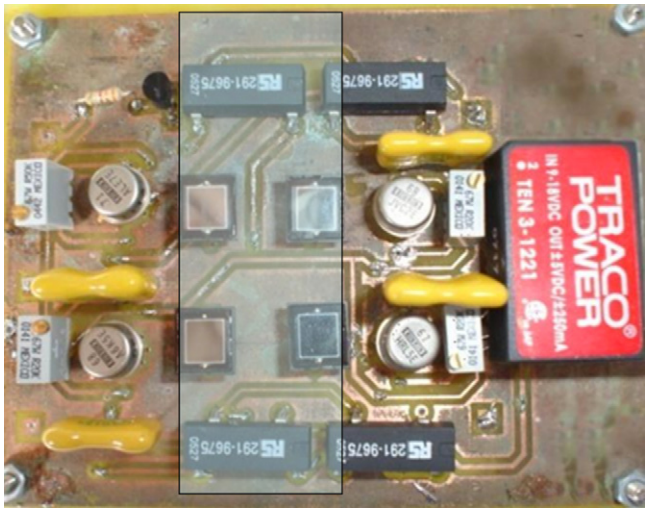


**Fig. 5.** Board with the integration circuit. The image also schematically shows housing of typical glass slide used in ELISA tests.

have the highest possible sensitivity. Output current is very low, about 200 pA. For this reason, an accurate resistance of 10 MΩ was selected to obtain a measurable voltage value. The potentiometer trimmers (10 kΩ to 1 MΩ) were inserted in order to suppress offset of the operational amplifier. Instead, Fig. 5 shows the board with the integrator circuit and enough available room for housing a typical glass slide used in ELISA tests. In this second architecture, the output current is integrated to obtain the charge in the capacitors. At the end of the integration time $T_{int}$, the capacitors are reset by means of transistor-driven reed-relays. A capacitor of exactly 1 nF is used because the output current of the sensors is very low.

The two boards, implementing two different detection circuits, were finally packaged in a metal box, in order to avoid electrical noise and to investigate possible integration in point-of-care systems. The box was also used to create a dark chamber to filter out the external light.

### 2.4. Chemiluminescence tests

Luminol molecule and hydrogen peroxide as oxidizing agent were chosen to test and validate the two developed circuits and the optical detector. These compounds can react with the horseradish peroxide (HRP), a very well know enzymes used in chemiluminescence assays, and produce the excited compound 3-APA (3-aminophthalate). The decay form a high to a lower energy level is responsible for the emission of light [19]. A microscope slide was spotted with 20 μL drops of a mixture of 45 μL of luminol reagent, 45 μL of oxidizing reagent and 10 μL of HRP covalently linked to an immunoglobulin M (IgM–HRP conjugate). After spotting, the slide was immediately positioned into the measuring chamber exactly in the positions showed in Figs. 4 and 5. Chemiluminescent signal was measured by means of three different systems: (i) the developed system based on current-to-voltage conversion, (ii) the developed system based on the integration circuit, (iii) a commercial available luminometer specifically developed for chemiluminescent applications (Luminoskan).

### 2.5. Validation on cancer marker detection

The sandwich immunoassay is prepared with the protocol reported by Collins et al. [20]. Primary antibody (the “capture” antibody) was immobilized onto a well plate. Antigen was then added and allowed to form a complex with the primary antibody. Unbound products were then removed by washing. A labelled sec-

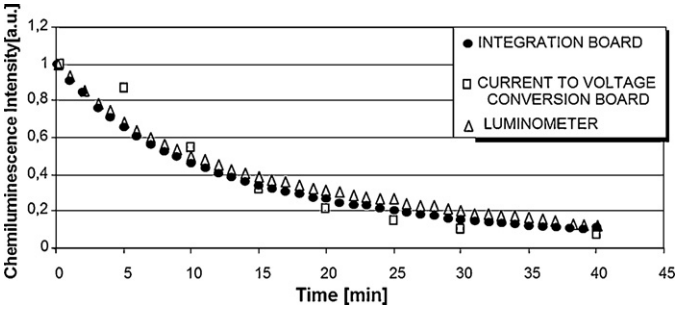


**Fig. 6.** Signals acquired with the two different detection circuits in comparison with those acquired using a commercially available luminometer.

ond antibody (the probe) was allowed to bind the antigen (from here the expression "sandwich"). This technique has two main advantages: the target antigen does not need to be purified prior to use, and the assay has very high specificity. Reagents of the reaction were Slides Superfrost Plus Menzel (used for electrostatic binding of the primary antibodies), Anti-Human IgM (Sigma I0140), Anti-Human IgM (μ-chain) peroxidase conjugate (Sigma A0420), Phosphate Buffer Saline pH 7.2 (buffer is used to maintain a constant pH in order to prevent proteins denaturation), PBS-Tween 0.05% – wash buffer (detergent), PBS–BSA 1% – block buffer (Bovine Serum Albumin is used to fill slide spaces not previously covered by the first antibody), Human Serum Samples, Western Lightning Chemiluminescence Reagent Plus (NEL105001EA PerkinElmer).

## 3. Results and discussion

### 3.1. Test of the two solutions

Fig. 6 depicts the behaviors of chemiluminescent signals vs. time for the three considered systems. All the curves show the typical exponential decay of chemiluminescent emission. The three different systems are compared with respect to different curve parameters. The estimation of chemiluminescence decay constants was firstly considered. A decay constant value equal to −0.055 was measured using the integration circuit board. This value is quite close to −0.049, the one obtained using the luminometer. On the other hand, a value equal to −0.079 was measured using the voltage-to-current board. This last value is not very close to of the previous one related to the luminometer. It means that sensitivity, detection limit, and dynamic range of the device are better for the integrator circuit, since the results are closer to those obtained with commercially available luminometers.

The signal-to-dark ratio is also estimated and compared. Values are calculated from the average of 10 different measurements at a sampling rate of 10 samples/s. As shown in Table 1, measurements for the dark-field results equal to 4.6 ± 1.3 pA in the case of voltage-to-current conversion, while the maximum luminescent signal is 320 ± 1.3 pA. In this case, the signal-to-dark ratio is about 70. Instead, the dark-field output in the case of the integration circuit is equal to 2.64 ± 0.92 pA with a maximum luminescent signal equal to 404 ± 0.92 pA. In this case, the signal-to-dark ratio is about 153. Therefore, the board based on integration circuit presents a signal-to-dark ratio twice higher than the value obtained with the current-to-voltage conversion.

**Table 1**
The different signals measured during tests to calculate the signal-to-dark ratios.

| | Current-to-voltage circuit | Integrator circuit |
|---|---|---|
| Dark current signal (pA) | 4.6 ± 1.3 | 2.64 ± 0.92 |
| Maximum current signal (pA) | 320 ± 1.3 | 404.00 ± 0.92 |

**Table 2**
The different signals measured during tests to calculate the signal-to-noise ratios.

| | Current-to-voltage circuit (mV) | Integrator circuit (pA) |
|---|---|---|
| Maximum noise signal | 0.4 ± 0.1 | 20 ± 1 |
| Maximum detected signal | 3.2 ± 0.1 | 404 ± 1 |

The signal-to-noise ratio is determined by characterizing the noise affecting maximum chemiluminescent signal. The output voltage was sampled with a sapling time of 100 ms in the case of the board based on current-to-voltage conversion. The average of the samples is considered as the maximum chemiluminescent signal, while the standard deviation is assumed as the noise affecting measurements. By following this method, the maximum detected signal was acquired in 3.2 mV with a noise of 0.4 mV, as shown in Table 2. Fig. 7 reports an example of the current acquired during these measurements. Therefore, the signal-to-noise-ratio is about 8 for the current-to-voltage conversion board. In the case of integration circuit, the capacitance charge is linear over 5 s. The photocurrent can be calculated as follows:

$$I_{ph} = C\frac{dV}{dT} \quad (7)$$

Then, the output voltage is sampled with a sampling time of 100 ms, in order to determine the signal-to-noise ratio; the slope between two subsequent samples is calculated; finally the mean value of the slopes was considered as the maximum chemiluminescent signal, while the standard deviation was considered as the noise. In this way, the maximum detected signal was 404 pA with a noise equal to 20 pA, as summarized in Table 2. Fig. 8 reports an example of the signal acquired during these measurements. Thus, a signal-to-noise ratio equal to 20 was obtained using the integration circuit board. All these results demonstrate that the board based on integrator circuit is better than the board based on current-to-voltage conversion. Hence, the board based on integrator circuit is chosen for the immunoassay tests.

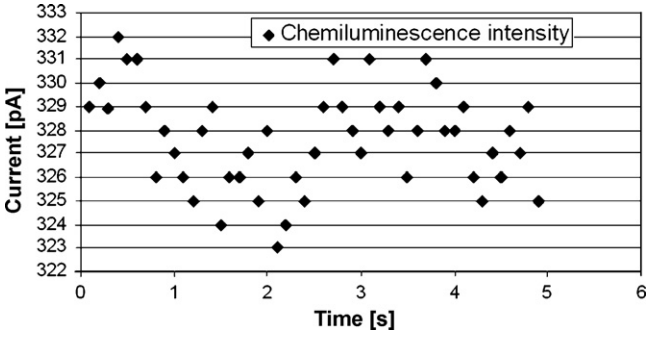


**Fig. 7.** Time trend of the chemiluminescent signal acquired using the current-to-voltage conversion.

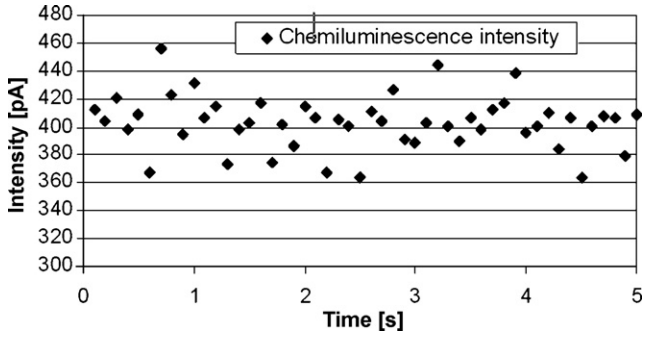


**Fig. 8.** Time trend of the chemiluminescent signal acquired using the integration circuit.

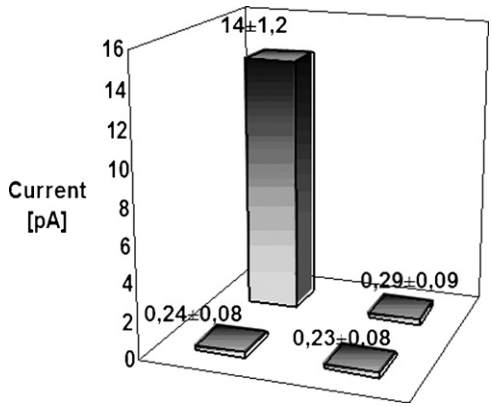


**Fig. 9.** Results obtained with an immunoassay on human serum for the detection of cancer markers.

### 3.2. Validation on cancer-assay

The integrator board was used to detect the chemiluminescence signal in an immunoassay sandwich in order to validate the system. The system is tested in human serum with a functionalization of antibodies for the inhibition of human immune complexes.

Two different reactions (immune assays) were performed on the same glass slide. In the first, a complete immune-complex sandwich was formed (this spot is able to glow chemiluminescence); in the second (the negative control spot) the absence of probe antigens assure no uptake of the target antigens, and, thus, the absence of chemiluminescence. Only non-specific molecular binding is expected from this spot. As further control, the areas of the third and fourth photodiodes are not covered with the solution, in order to only measure dark currents. Just prepared slides were immediately inserted into the measuring chamber, being careful with the alignment between the photodiodes array and the functionalized spots in the slide. Then, the different photodiodes responses were acquired and compared. The output voltage of the system was sampled with an interval of 100 ms, as was done in the previous test. Fig. 9 shows the experimental results. The photosignal returned a maximum current value of $14 \pm 1.2$ pA (sites top left) in the case of measurements from the spot where immune complexes were formed. On the contrary, when the immune complexes were not formed (site top right), the obtained value (290 fA) was close to of the one obtained in the dark field (242 fA as average from bottom sites). The signal from the first site also decreases exponentially over the time, approaching the dark-field signal-value within 5 min, accordingly with chemiluminescence decay. These currents signals were estimated by the acquired output voltages. These voltages were measured equal to $14 \pm 1.2$ mV/s on spot containing the matching molecules (the full sandwich of probes and targets), equal to 290 μV/s on spot containing the molecular control (spot without primary antibodies), and equal to 242 μV/s on spots without chemistry (used to measure the dark currents).

The maximum chemiluminescent signal obtained in the immunoassay with human serum (Fig. 9) is smaller than those acquired in the experiments with the luminol alone (Fig. 8). This is due to the number of enzymes immobilized onto the slide surface, which affects the total emission intensity.

## 4. Conclusion

In this paper the feasibility of a devices based on low-cost off-the-shelf components is investigated for parallel ELISA assay. Data from two different circuit architectures (current-to-voltage conversion and current integration) are compared, in order to identify the best one. The two proposed architectures are developed on PCB and packaged with a portable camerafor point-of-care applications. The best results were obtained with the architecture based on current integration. This circuit is validated with immunosensor assay. A signal equal to $14 \pm 1.2$ pA is measured, corresponding to chemiluminescent from spots where the immune complexes were formed. A signal of 290 fA is instead measured from those spots where the immune complexes were not formed. Signals from spots with non-specific molecular binding were very close to those obtained in dark-field conditions. The developed system also detected the exponential decay of chemiluminescent emissions. Hence, the present study demonstrated the feasibility of the proposed system for the development of point-of-care devices in immune assay. This work paves the way to portable, fast, sensitive, and very low-cost point-of-care devices for early detection of cancer markers using ELISA tests. Even in prototype form, the total cost of the system, was 52 times lower than commercially available luminometers, and 75 times lower than the high-sensitivity scanners.

## Acknowledgements

The authors acknowledge the Bank of Samples in Venice Scientific Park (Venice, Italy) for human serum from liver-cancer patients. Cristina Boero is acknowledged for proofreading of the manuscript. A part of this work has been presented at the IEEE Conference on Biomedical Circuits and Systems, BioCAS 2009, Beijing, 26–28 November 2009.

## References

[1] F. García Sánchez, A. Navas Díaz, C. Delgado Téllez, M. Algarra, Determination of asulam by fast stopped-flow chemiluminescence inhibition of luminol/peroxidase, Talanta 77 (2008) 294–297.
[2] A.M. Jiménez, M.J. Navas, Chemiluminescence detection systems for the analysis of explosives, J. Hazard Mater. 106A (2004) 1–8.
[3] M.F. Sawalha, M.K. Sengupta, S.-I. Ohira, A.D. Idowu, T.E. Gill, L. Rojo, M. Barnes, P.K. Dasgupta, Measurement of soil/dust arsenic by gas phase chemiluminescence, Talanta 77 (2008) 372–379.
[4] Q.-L. Zhang, J. Li, T.-T. Ma, Z.-T. Zhang, Chemiluminescence screening assay for diethylstilbestrol in meat, Food Chem. 111 (2008) 498–502.
[5] D. Ivnitski, I. Abdel-Hamid, P. Atanasov, E. Wilkins, Biosensors for detection of pathogenic bacteria, Biosens. Bioelectron. 14 (1999) 599–624.
[6] H. Eltoukhy, K. Salama, A. El Gamal, A 0.18-μm CMOS bioluminescence detection lab-on-chip, IEEE J. Solid State Circuits 41 (2006) 651–662.
[7] C. Dodeigne, L. Thunus, R. Lejeune, Chemiluminescence as diagnostic tool. A review, Talanta 51 (2000) 415–439.
[8] L.J. Kricka, Clinical applications of chemiluminescence, Anal. Chim. Acta 500 (2003) 279–286.
[9] G.J. Kost (Ed.), Principles and Practice of Point-of-Care Testing, Lippincott Williams and Wilkins, Philadelphia, 2002, pp. 3–12 (Chapter 1).
[10] A. Lyapandra, M. Karpinskyy, Electronic devices for chemiluminescence assay, in: Conference TCSET'2004, Lviv-Slavsko, Ukraine, February 24-28, 2004.
[11] G.C. Fiaccabrino, P. Zwahlen, P. Thikbaud, G.A. Racine, N.F. de Rooij, M. Koudelka-Hep, On Chip detection of electrogenerated chemiluminescence of Ru(bpy)—at Pt interdigitated microelectrode arrays, in: International Conference on Solid-State Sensors and Actuators, Transducers'97, Chicago, June 16–19, 1997.
[12] A.C. Pimentel, A.T. Pereira, V. Chu, D.M.F. Prazeres, J.P. Conde, Detection of chemiluminescence using an amorphous silicon photodiode, IEEE Sens. J. 7 (2007) 415–416.
[13] T.-B. Xin, S.-X. Liang, X. Wangb, H. Li, J.-M. Lin, Determination of estradiol in human serum using magnetic particles-based chemiluminescence immunoassay, Anal. Chim. Acta 27 (2008) 277–284.
[14] M. Zoli, D. Magalotti, G. Bianchi, C. Guelli, G. Marchesini, E. Pisi, Efficacy of a surveillance program for early detection of hepatocellular carcinoma, Cancer 78 (1996) 977–985.
[15] S. Carrara, V. Bhalla, C. Stagni, L. Benini, A. Ferretti, F. Valle, A. Gallotta, B. Riccò, B. Samorì, Label-free cancer markers detection by capacitance biochip, Sens. Actuators B: Chem. 136 (2009) 163–172.
[16] W. Xu, Y. Wei, D. Xing, Q. Chen, S. Luo, Quantification of human serum albumin by highly sensitive chemiluminescence method, in: Proceedings of the 2007 International Conference on Complex Medical Engineering, IEEE/ICME 2007, Beijing, China, July 2–5, 2007.
[17] S. Carrara, V. Bhalla, C. Stagni, B. Samorì, Nanoscale film structure related to capacitive effects in ethylene-glycol monolayers, Surf. Sci. 603 (2009) L75–L77.
[18] J.M. Goddard, J.H. Hotchkiss, Polymer surface modification for the attachment of bioactive compounds, Prog. Polym. Sci. 32 (2007) 698–725.

[19] I.G.K. Turner, Measurement of light from chemical or biochemical reactions, in: N. Van Dyke, C. Van Dyke, K. Woodfork (Eds.), Bioluminescence and Chemiluminescence: Instruments and Applications, 1985.
[20] F. Collins, M. Morgan, A. Patrinos, The human genome project: lessons from large-scale biology, Science 300 (2003) 286–290.

## Biographies

**Paquale Grosso** was born in Belvedere Marittimo, Italy, on June 27, 1982. In October 2007, he received the degree in electronic engineering from the University of Bologna, Italy, working on low-cost systems for chemiluminescent detection. He also worked on CMOS design of potentiostats for electrochemical bio-detection. He now works with Alten Italia s.p.A. Bologna, Italy.

**Sandro Carrara** graduated in physics from the University of Genoa, Italy, in 1990 and received the Ph.D. degree in biochemistry and biophysics from the University of Padoa, Italy, in 1998. He is Senior Research Scientist in the Ecole Polytechnique Federale de Lausanne and Professor of nano-bio-sensing and micro/nano interfaces at the Department of Electrical Engineering and Biophysics (DIBE) of the University of Genoa. He was a Professor in biophysics in University of Genoa and a Professor of nanobiotechnology in University of Bologna. His research interests are interdisciplinary including areas in biophysics, nanotechnology, electronic engineering, circuits and system design, and system integration. He has published more than 70 papers and several book chapters. He won several prices for best contributions in several international conferences. He was a member of the User Committee of the ELETTRA Synchrotron, and scientific leader of a National Research Program in the field of nanotechnology. He was a chair of special sessions in several IEEE international conferences. He is an associate editor of the IEEE Transactions on Biomedical Circuits and Systems, and of the IEEE Sensors Journal. He is also a referee of more than 10 international journals in the field of bio-sensing systems and circuits.

**Claudio Stagni** was born in Pavullo, Italy, on December 17, 1977. He received the degree in electrical engineering from the University of Bologna, Italy, with a thesis on "Capacitance measurements to detect DNA hybridization", in July 2002. Since 2003, he has been working toward the Ph.D. degree at the same university on design and test of low-cost biosensors. In 2004, he was with Infineon Technologies, Munich, Germany, where he worked in the field of CMOS DNA sensors. Until September 2007, he has developed and tested new low-cost DNA or Protein biosensor. Now, he works as hardware/firmware designer at Arenagiochi s.r.l. He has published more than 15 papers and a book chapter on electronic circuit for biomedical applications.

**Luca Benini** is Full Professor at the Department of Electrical Engineering and Computer Science (DEIS) of the University of Bologna. He also holds a visiting faculty position at the Ecole Polytechnique Federale de Lausanne (EPFL). He received a Ph.D. degree in electrical engineering from Stanford University in 1997. Dr. Benini's research interests are in the design of system-on-chip platforms for embedded applications. He is also active in the area of energy-efficient smart sensors and sensor networks for biomedical and ambient intelligence applications. He has published more than 500 papers in peer-reviewed international journals and conferences, four books and several book chapters.

He has been general chair and program chair of the Design Automation and Test in Europe Conference. He is an Associate Editor of several international journals, including the IEEE Transactions on Computer Aided Design of Circuits and Systems and the ACM Transactions on Embedded Computing Systems. He is a Fellow of the IEEE and a member of the steering board of the ARTEMISIA, the European Association on Advanced Research and Technology for Embedded Intelligence and Systems.